Computational Models in Nano–Bio–Electronics:

Simulation of Ionic Transport in Voltage Operated Channels

Massimo Longaretti[1,♯], Giovambattista Marino[1,♯], Bice Chini[2],

Joseph W. Jerome[3], Riccardo Sacco[4,*]

[1] Scientific Collaborator,

Politecnico di Milano, Piazza Leonardo da Vinci 32, 20133 Milano, Italy.

E-mail: ionici@mate.polimi.it.

[2] CNR Institute of Neuroscience Cellular and Molecular Pharmacology Section,

via Vanvitelli 32, 20129 Milano, Italy.

Tel.: +39 02 5031 6958, E-mail: B.Chini@in.cnr.it.

[3] Department of Mathematics, Northwestern University,

2033 Sheridan Road, Evanston, IL 60208-2730, USA.

Tel.: +01 847 491 5575, E-mail: jwj@math.northwestern.edu.

[4] Dipartimento di Matematica "F. Brioschi", Politecnico di Milano,

via Bonardi 9, 20133 Milano, Italy.

Tel.: +39 02 2399 4540, E-mail: riccardo.sacco@mate.polimi.it.

[♯] This author contributed equally to the work.

[*] Corresponding author.

Abstract

In this article, a novel mathematical and computational model is proposed for the numerical simulation of Voltage Operated ionic Channels (VOC) in Nano–Bio–Electronics applications. This is a first step towards a multi–physics description of hybrid bio–electronical devices such as bio–chips. The model consists of a coupled system of nonlinear partial differential equations, comprising a Poisson-Nernst-Planck system to account for electro-chemical phenomena, and a Navier–Stokes system to account for fluid–mechanical phenomena. Suitable functional iteration techniques for problem decoupling and finite element methods for discretization are proposed and discussed. Numerical results on realistic VOCs illustrate the validity of the model and its accuracy by comparison with relevant computed channel equivalent electrical parameters with measured data.

Keywords: Nanotechnology; hybrid bio–artificial systems; ionic–electrical coupling; ionic channels; mathematical modeling; numerical simulation.

1 Introduction

In this article, we deal with the study of charge transport in Voltage Operated ionic Channels (VOCs) [11, 1] for application in Bio–Electronics [20, 25]. The differential mathematical model of a VOC consists of a coupled system comprising a Poisson-Nernst-Planck (PNP) system for the electro–chemical part [24, 21, 2], and of a Navier–Stokes (NS) system for the fluid-mechanical part [17]. The highly nonlinear structure of the system has a strong resemblance to the hydrodynamical equations used to model charge flow in semiconductor devices [12]. Such resemblance suggests adopting proper functional iteration techniques for system decoupling and linearization [12], as well as accurate and stable finite element formulations, combining exponential fitting, Mixed-Hybrid (MH) and Discontinuous Galerkin (DG) approaches, for the numerical approximation of the resulting linearized differential subproblems [3, 4, 7]. All of these advanced mathematical techniques are the basic ingredients of a sophisticated computational tool, that has been developed for the two–dimensional numerical simulation of VOCs and, in perspective, of complex coupled hybrid bio-artificial systems such as Nanoscale Biological Chips (NBC) [20, 25].

A summary of the contents of the article is as follows. In Sect. 2 a schematical example of an NBC device and of its functional properties is provided. Then, the attention is focused on the characterization of ionic charge flow that is exchanged between the biological (cell) and electronic component of the NBC device throughout the Voltage Operated Channels (VOCs) that are largely present on the cell membrane. In Sect. 3 the mathematical model of charge transport in a single VOC, including electro–chemical and fluid–mechanical forces, is discussed in detail, while in Sect. 4 the functional and numerical techniques adopted for linearization and discretization are briefly illustrated. Finally, the physical validity of the model, and the accuracy

of computational techniques are illustrated in Sect. 5 on the numerical simulation of a realistic single VOC under several working conditions and on the comparison with relevant computed electrical equivalent parameters with measured data. Some concluding remarks and prospective directions are addressed in Sect. 6.

2 An Example of A Hybrid Device: The EOSFET

This section has the aim of introducing the simplest example of a bio-chip, the so-called EOSFET (Electrolyte Oxide Field Effect Transistor), a schematic of which is shown in Fig. 1. The

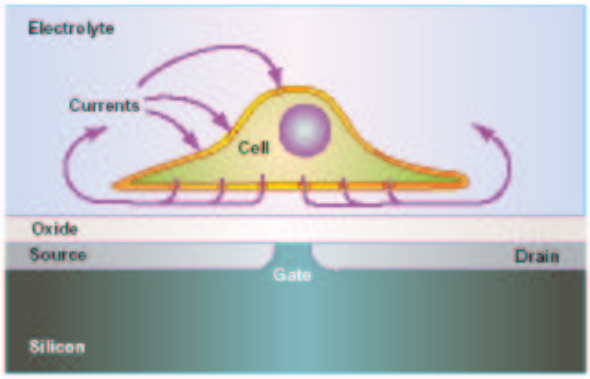

Figure 1: A coupled hybrid device (reprinted from [20]).

EOSFET structure is a transistor device where the gate contact is constituted by an electrolyte solution instead of a metal interconnection, as in a standard semiconductor technology. Integration of cell and chip is made possible by proper control of the flow of *ionic charges* exchanged between the cell and the semiconductor component, in such a way that the hybrid device can function under two different modes of operation. In the first mode, the cell gates the transistor and regulates the electronic current flowing into the transistor conducting channel. In the second mode, which is the reversal case, the cell acts as the receiver of a signal coming from a microelectronical network (see also [9], [20] and [25]).

The structural difference between the EOSFET and the conventional MOSFET (Metal-Oxide Field Effect Transistor) device implies a radical change in the nature of the charges which control the transistor. In the case of a MOSFET, the conducting channel is gated by the electric field generated by electrons in the gate contact, while in the case of an EOSFET the gating process is operated by ionic charges coming from the cell towards the semiconductor.

Ionic charges are injected through thin passages, called *Voltage Operated ionic Channels (VOCs)*, which are largely present on the cellular membrane [11]. Ionic channels are the connection between the cytoplasm and the extra-cellular environment, and:

- *regulate and maintain* the dynamical electro-chemical equilibrium between the cell-surrounding environment and the intracellular milieu;
- *supervise* fundamental biological processes, such as nervous transmission, muscle contractivity and secretion;
- are characterized by a *specific geometry* and *selectivity and gating properties.*

A first step towards the implementation of a reliable and effective simulation tool of an EOSFET device consists of devising:

- Mathematical models for charge transport in ionic channels in the presence of large gradients of ion concentration and action potential (see [11, 14, 13, 12, 5]).
- Efficient functional iteration techniques [12] and accurate and stable finite element methods [3, 4], for system decoupling and linearization and subsequent numerical discretization.

3 Mathematical Model for Ionic Channels

In this section, we discuss the mathematical model for the electrical and fluid description of transport in a *single ionic channel*, and the boundary and initial conditions to be supplied to close the differential problem.

3.1 The Ingredients of the Model

Ionic charges flow throughout the channel in a moving aqueous electrolyte medium and subject to the following forces:

- *electrical* or *drift* forces;
- *thermodynamical* or *diffusion* forces;
- *fluid-mechanical* forces.

The electrical force is due to the voltage difference between the inside and the outside of the cell. The diffusion force is due to the concentration drop across the membrane and obeys the standard Fick's law. The fluid-mechanical force is due to the presence of a fluid in motion (the aqueous electrolyte) under the action of a given pressure difference across the channel and of the electric pressure exerted by the flowing ions. As a matter of fact, biological arguments show a significant decrease of (effective) diffusion between the end regions of the channel and the wider regions (cf. Fig. 2). This reduction of the diffusive mechanism gives rise to a highly convection–dominated flow in the narrow regions of the channel, which in turn requires appropriate modeling. To properly describe the above three kinds of forces, two different sets of PDEs must be considered:

1. the **Poisson-Nerst-Planck** (PNP) equations;

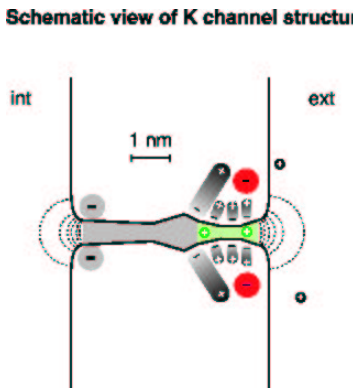

Figure 2: Ionic transport in and out of a single K^+ channel (reprinted from [10]).

2. the **Navier-Stokes** (NS) equations.

The PNP system of equations accounts for the electrical and diffusion forces, while the NS system of equations accounts for the fluid-mechanical forces. The two sets of PDEs constitute a highly nonlinear coupled problem, and suitable solution algorithms are needed to compute a consistent solution. The presence of the Navier-Stokes equations in the model is a novel contribution of the present work, compared to existing literature [5, 21, 2, 8, 10]. Previous examples of modeling and simulation of ionic flow in biological channels can be found in [24],[5], [21, 2], [8] and [6].

3.2 The Scaled PNP Equations

The PNP system in scaled form reads:

$$\begin{cases} \sigma_i \dfrac{\partial n_i}{\partial t} + \operatorname{div} \boldsymbol{J}_i = 0 \\ \lambda^2 \operatorname{div} \boldsymbol{E} = \displaystyle\sum_{i=1}^{M} \sigma_i n_i + d \\ \boldsymbol{J}_i = (\mu_i \boldsymbol{E} + \boxed{\sigma_i \alpha \boldsymbol{u}}) n_i - \sigma_i \mu_i \boldsymbol{\nabla} n_i \\ \boldsymbol{E} = -\boldsymbol{\nabla} \varphi. \end{cases} \tag{1}$$

The variables of the system are the concentration n_i of the i-th ionic species, with $i = 1, \ldots, M$, $M \geq 1$, the associated current density $\boldsymbol{J}_i$ and the electric field $\boldsymbol{E}$, that is related to the electric

potential φ by $(1)_4$. The velocity of the electrolyte fluid $\boldsymbol{u}$ is assumed here to be a given function. The quantities σ_i and μ_i, denote the sign and the mobility of the i-th ionic species, respectively. The function d is a given function which represents a fixed concentration in the channel. We notice that a classical DD-like constitutive equation is used for the current density $\boldsymbol{J}_i$ in $(1)_3$, with the addition of a boxed term $\sigma_i\,\alpha\,\boldsymbol{u}\,n_i$, which acts as a correction to the drift term and is responsible for the coupling between electro–chemical forces and fluid–mechanical forces in (1). Two parameters, λ and α, enter the scaled PNP system (1). The first parameter is defined as $\lambda = \dfrac{\left(\dfrac{\varepsilon_e\,\overline{\varphi}}{q\,\overline{n}}\right)^{1/2}}{\overline{x}} \equiv \dfrac{l_e}{\overline{x}}$, where $\overline{\varphi}$, $\overline{n}$ and $\overline{x}$ are the scaling factors for potential, concentrations and spatial coordinates, respectively, while q and ε_e are the electron charge and the electrolyte permittivity, respectively. The parameter λ can be interpreted as a *scaled Debye length* [15] of the electrolyte. It is relevant to observe that if $\lambda^2 \ll 1$, the PNP system exhibits a singularly perturbed character (see [18]), and the corresponding solutions may exhibit internal and/or boundary layers, depending on the form of d and the given boundary conditions. In the problem at hand, a typical value of the above parameter is $\lambda^2 = 2 \cdot 10^{-2}$, which demonstrates that the PNP problem is singularly perturbed. The second parameter is defined as $\alpha = \dfrac{\overline{u}_{fl}}{\overline{u}_{el}}$, where $\overline{u}_{fl}$ and $\overline{u}_{el}$ are the scaling factors of the fluid velocity (in the NS model) and of the drift velocity (in the PNP model), respectively. It is relevant to notice that α is a multiplication factor of the coupling term between the electro–chemical and fluid-mechanical subsytems, and in the problem at hand we have $\alpha \simeq 56$.

3.3 The scaled NS Equations

The scaled NS equations in conservative form read:

$$\begin{cases} \operatorname{div} \boldsymbol{u} = 0 \\ \dfrac{\partial \boldsymbol{u}}{\partial t} + \boldsymbol{div}(\boldsymbol{u} \otimes \boldsymbol{u}) - \boldsymbol{div}\ \underline{\underline{\sigma}}(\boldsymbol{u}, p) = \boxed{\beta \sum_{i=1}^{M} \sigma_i n_i \boldsymbol{E}} \\ \underline{\underline{\sigma}}(\boldsymbol{u}, p) = \dfrac{2}{Re} \underline{\underline{\varepsilon}}(\boldsymbol{u}) - p \underline{\underline{\delta}} \\ \underline{\underline{\varepsilon}}(\boldsymbol{u}) = \dfrac{1}{2}(\boldsymbol{\nabla u} + (\boldsymbol{\nabla u})^T), \end{cases} \tag{2}$$

where $\underline{\underline{\sigma}}$ is the stress tensor, $\underline{\underline{\varepsilon}}$ is the strain rate tensor, $\boldsymbol{u}$ is the fluid velocity and p is the pressure. The boxed term at the right-hand side of the momentum balance equation $(2)_2$ is the electric pressure exerted by the ionic charges on the electrolyte fluid, and is responsible for the coupling between the NS system (2) and the PNP system (1). Two parameters, β and Re, enter the scaled system (2). The first parameter is defined as $\beta = \dfrac{q\ \overline{n}\ \overline{E}}{\overline{f}_{fl}}$, where $\overline{E}$ is the scaling factor for electric field and $\overline{f}_{fl} = \rho_e\ \overline{u}_{fl}^2\ /\ \overline{x}$, ρ_e being the fluid density. It is relevant to notice that β is a multiplication factor of the coupling term between the fluid-mechanical and electro–chemical subsytems, and in the problem at hand we have $\beta \simeq 10$. The second parameter is the *Reynolds number* of the electrolyte fluid (see [22]), and is defined as $Re = \dfrac{\overline{x}\ \overline{u}_{fl}}{\nu_e}$, where $\nu_e = \mu_e/\rho_e$ is the kinematic viscosity of the fluid, μ_e denoting its shear viscosity. Using realistic data, the estimated value of Re is $\mathcal{O}(10^{-1})$, which means that the fluid can be considered in the fully laminar regime. This allows simplifying the fluid-mechanical model into a much easier Stokes (ST) problem, where the nonlinear convective term $\boldsymbol{div}(\boldsymbol{u} \otimes \boldsymbol{u})$ is neglected. By doing so, the computational work of the numerical solver is reduced, still retaining a sound physical accuracy.

3.4 Geometry, Boundary and Initial Conditions

In this section, we define the computational domain and provide proper boundary and initial conditions for the PNP and ST subsystems. With this aim, Fig. 3 (left) shows a 2D cross–section of a single ionic channel, while Fig. 3 (right) shows the simplified geometrical description of the physical environment adopted in the present work.

From now on, we denote by $\Omega \subset \mathbb{R}^2$ the computational channel domain, and by Γ its boundary, with $\Gamma = \Gamma_1 \cup \Gamma_2 \cup \Gamma_3 \cup \Gamma_4$. For each boundary segment Γ_j, $j = 1, \ldots, 4$, an appropriate boundary condition (of Dirichlet, Neumann or Robin type) can be imposed (see [22]), according to either the user need or physical adherence.

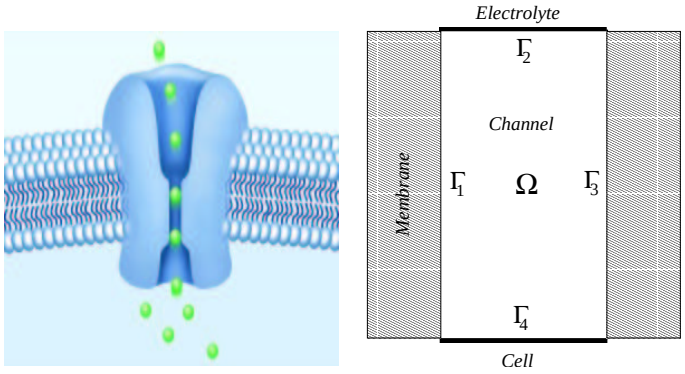

Figure 3: A 2D cross-section of the membrane and of a single ionic channel (left). Simplified geometrical description (right).

We also denote by $T_{fin} > 0$ the (scaled) duration of the temporal evolution of system (1)–(2), and we set $T_{fin} = +\infty$ if steady–state conditions are investigated.

3.4.1 Boundary and Initial Conditions for the PNP system

The boundary and initial conditions for the PNP system (1) can be written as follows:

$$\begin{cases} \varphi = \overline{\varphi}_2 & \text{on } \Gamma_2 \\ \varphi = \overline{\varphi}_4 & \text{on } \Gamma_4 \\ \nabla\varphi \cdot \boldsymbol{n}_\Gamma = 0 & \text{on } \Gamma_1 \cup \Gamma_3 \\ n_i = \overline{n}_{i,2} & \text{on } \Gamma_2, \\ n_i = \overline{n}_{i,4} & \text{on } \Gamma_4, \\ \boldsymbol{J}_i \cdot \boldsymbol{n}_\Gamma = \sigma_i \overline{v}_{i,\Gamma}(n_i - \overline{n}_{i,\Gamma}) & \text{on } \Gamma_1 \cup \Gamma_3, \\ n_i(\boldsymbol{x}, 0) = n_i^0(\boldsymbol{x}) & \text{in } \Omega, \end{cases} \tag{3}$$

where $\overline{\varphi}_i$ is the electric potential of side i, in particular of the cytoplasm and of the extracellular mean, $\overline{n}_{i,j}$ is a given concentration of the ionic species i (intracellular and extracellular) on side Γ_j, while $n_i^0(\boldsymbol{x})$ is the initial concentration in the ionic channel at time $t = 0$ for the i-th ionic species. Conditions $(3)_{1-2}$ enforce a given voltage drop across the channel, conditions $(3)_{4-5}$ enforce a given concentration gradient across the channel, and condition $(3)_3$ express the fact that the channel is electrically self–contained. Condition $(3)_6$ expresses the possibility for an ionic current to flow (by osmosis) from the membrane into the ionic channel and to add it to the electrical current in the channel. The inclusion of such a boundary condition in the PNP formulation increases the portability of the model to other possible uses and applications where an osmotic component of the current might be of interest (for example, bio-hydraulics, micro-and-nano fluidics, plasma-dynamics, see [13]).

3.4.2 Boundary and Initial Condition for the NS System

The boundary and initial conditions for the NS (ST) system are:

$$\begin{cases} \boldsymbol{u} = 0 & \text{on } \Gamma_1 \cup \Gamma_3 \\ \underline{\underline{\sigma}}(\boldsymbol{u}, p)\boldsymbol{n}_\Gamma = \overline{p}_2 \boldsymbol{n}_\Gamma & \text{on } \Gamma_2 \\ \underline{\underline{\sigma}}(\boldsymbol{u}, p)\boldsymbol{n}_\Gamma = \overline{p}_4 \boldsymbol{n}_\Gamma & \text{on } \Gamma_4 \\ \boldsymbol{u}(\boldsymbol{x}, 0) = \boldsymbol{u}^0(\boldsymbol{x}) & \text{in } \Omega. \end{cases} \tag{4}$$

Relation $(4)_1$ is the adherence condition, relations $(4)_2$ and $(4)_3$ enforce a pressure drop between the inside and the outside of the cell, while relation $(4)_4$ states the fact that at time $t = 0$ the velocity of the fluid is known in all the domain (typically, we set $\boldsymbol{u}^0(\boldsymbol{x}) = \boldsymbol{0}$).

4 Functional Iterations and Numerical Approximation

In order to deal with the numerical approximation of the PNP/ST differential system discussed in the previous sections, we need to introduce a suitable iterative procedure which allows the successive solution of the two model sub–blocks (1) and (2). Then, proper finite element formulations must be used for the discretization of the resulting decoupled problems.

4.1 A Staggered Algorithm

The staggered algorithm for the successive solution of the PNP and ST subsystems is organized as follows. For each time level t^m, set $n_i^{(0)} = n_i^m$, $\boldsymbol{E}^{(0)} = \boldsymbol{E}^m$ and $\boldsymbol{u}^{(0)} = \boldsymbol{u}^m$. Then, for each $k \geq 0$, solve successively:

- a linearized PNP system with a given velocity field $\boldsymbol{u}^{(k)}$. This provides in output the updated densities $n_i^{(k+1)}$ and electric field $\boldsymbol{E}^{(k+1)}$;
- a linear ST system with a given electric field $\boldsymbol{E}^{(k+1)}$. This provides in output the updated velocity $\boldsymbol{u}^{(k+1)}$;

- let k^* be the value of k at which self–consistency is achieved for the time level t^m. Then, set $n_i^{m+1} = n_i^{(k^*)}$, $\boldsymbol{u}^{m+1} = \boldsymbol{u}^{(k^*)}$, $\boldsymbol{E}^{m+1} = \boldsymbol{E}^{(k^*)}$, and then set $t = t^{m+1}$.

Each decoupled sub–block of the above iteration can be solved by resorting to suitable linearization. In the case of the PNP system, the classical Gummel's map that is widely employed in contemporary semiconductor device simulation can be profitably employed [12]. In the case of possible convective dominance in the electrolyte fluid motion, an Oseen–type formulation can be adopted to treat the nonlinear term in the momentum balance equation (see [23]).

4.2 Finite Element Approximation

As previously anticipated, the solutions of the PNP and ST subsystems can exhibit a markedly singularly perturbed character (see [12]). Moreover, due to the common structure in divergence form, conservation of flux and tensor quantities is an important issue for the computed solution. As a matter of fact, it is well–known that flux/stress post–processing may lead to a degradation in the accuracy, due to numerical differentiation. Moreover, standard displacement–based finite element formulations do not provide interelement continuity of normal flux and stress, which constitutes a violation of the action–reaction principle on the discrete level. Therefore, in view of the finite element approximation of the PNP and ST subsytems, we use:

- Mixed–Hybrid finite element formulations that allow a flexible enforcement of the constitutive relations for vector and tensor quantities, as well as of the associated conservation and equilibrium equations (see [4]);

- Exponentially Fitted Mixed Finite Volume schemes (see [19, 3]) in the discretization of the continuity equations in the PNP model. In the case where a full NS problem must be solved for the fluid motion, a suitable Discontinuous Galerkin upwinding treatment of the

convective terms in the NS system should be adopted (see [7]).

5 Numerical Results

In this section, we provide a validation of the PNP/ST model and of the related computational procedures, in the simulation of a realistic single K^+ ionic channel under several working conditions. The following assumptions are introduced in all the subsequent numerical experiments:

1. the considered ionic channel is *ideally selective*, which means that ionic transport of only one species is allowed, while ionic transport of any other species is prohibited;

2. only *static computations* are performed, because gating and action potentials act on the scale of milliseconds, whereas transient phenomena in channels and devices seem to occur on the order of nanoseconds or even smaller units (see [14], Chapt. 3).

According to a *hierarchical* approach, we start studying the static current-voltage (I-V) characteristics of the single VOC using the sole PNP model in Sect. 5.1, because this allows a more immediate calibration of the model parameters through a direct comparison with available results in the literature [14, 9]. Then, the complete PNP-ST model is used in Sect. 5.2 for simulation and comparison. In all the reported numerical experiments, the channel current I_{ch}, expressed in A, is computed as $I_{ch} = I_{ch,2D}\, W$, where $I_{ch,2D}$ is the current per unit length flowing throughout the 2D domain Ω, expressed in $A\, m^{-1}$, and W is the width W of the channel in the direction perpendicular to the domain itself. In our tests, we take $W = 2\, nm$, which is equivalent to assuming that the channel has a square cross-section of $2 \times 2\, nm^2$.

5.1 I-V Characteristics Computed With the PNP model

The values of intra and extra-cellular K^+ ionic concentration, and the values of ionic mobility used in the simulations are $\overline{n}_4 = 400\,mM$, $\overline{n}_2 = 20\,mM$ and $\mu = 7.2 \cdot 10^{-8}\,m^2V^{-1}s^{-1}$, respectively [16]. It is important to notice that in the mentioned reference, mobility is evaluated by performing a molecular dynamics simulation, assuming an *infinite dilution* for the ions, and then neglecting *interionic interactions*. Moreover, the viscous nature of the force exerted by the electric field on the ions is due to the presence of the dielectric and hydrodynamical frictions, where the electrolyte dielectric permittivity is that of water ($\varepsilon_r = 80.4$). Two different triangulations of the channel domain are used, one consisting of 288 elements (T1), the other consisting of 1152 elements (T2). The voltage drop across the membrane ranges from $-120\,mV$ to $20\,mV$.

Before discussing the numerical results, it is useful to provide an equivalent representation for the ionic current density $\boldsymbol{J}$. Setting $\boldsymbol{u} = \boldsymbol{0}$ in $(1)_3$, the ionic flux density can be written in the following gradient form

$$\boldsymbol{J}_i = -\mu_i\, n_i\, \nabla \varphi_{n_i}, \tag{5}$$

where φ_{n_i} is the *electrochemical potential* associated with the i-th ionic species.

A first check on the accuracy of the simulation results consists of comparing the theoretical value of the *Nernst potential* V_N with its computed estimate, V_N being defined as the potential drop across the channel in correspondance of which $\boldsymbol{J} = \boldsymbol{0}$, this implying from (5) that the electrochemical potential φ_n is a constant quantity in the channel. The expression for V_N is (see [14], Sect. 2.6.1)

$$V_N = -V_{th}\, \ln\left(\frac{\overline{n}_4}{\overline{n}_2}\right) \simeq -80\,mV, \tag{6}$$

where V_{th} is the thermal voltage equal approximately to $26\,mV$ at room temperature.

This is shown in Fig. 4, which represents the I-V curve of the channel computed on T1, where the black circle indicates the (approximate) computed value of V_N. The obtained result is in very good agreement with the predicted value (6), with a discrepancy of 5 percent. A better resolution can be obtained by performing computations on the finer grid T2. A second significant

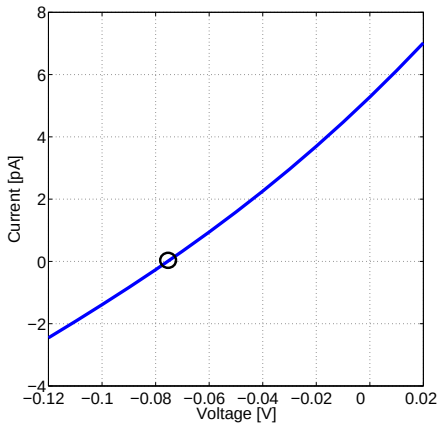

Figure 4: I-V curve of a single K^+ channel.

check on the accuracy of the simulation concerns the evaluation of the channel conductance g_{ch}, which is an equivalent electrical parameter of the channel [9], and is defined as

$$g_{ch} = \frac{d\,I_{ch}}{d\,V_m} \tag{7}$$

where $d\,V_m$ denotes an infinitesimal voltage drop across the membrane. Assuming, as usual in biological applications (see [14]), as reference potential the one of the extracellular environment, an extrapolation of g_{ch} from Fig. 4 yields $g_{ch} = 67.6\,pS$, which is in excellent agreement with tabulated ranges of measured data in [9] and with numerical simulations performed in [10]. A third concluding check on the accuracy of the simulation concerns the computation of the electrochemical potential in two different biasing conditions. The aim is to verify that the profile of φ_n tends to a constant value, as soon as the applied potential drop gets closer to the Nernst

potential V_N, in accordance with the flux density constitutive equation (5). Fig. 5 shows the distributions of φ_n in the case of $\Delta\,\varphi_{4,2} = -\Delta\,\varphi_{2,4} = 20\,mV$ (left) and $\Delta\,\varphi_{4,2} = -80\,mV$ (right), this latter biasing condition being very close to the theoretical value of V_N. Comparing the two plots, it can be seen that in the second case the variation of φ_n is negligible compared to the first case, consistently with the previous expectations.

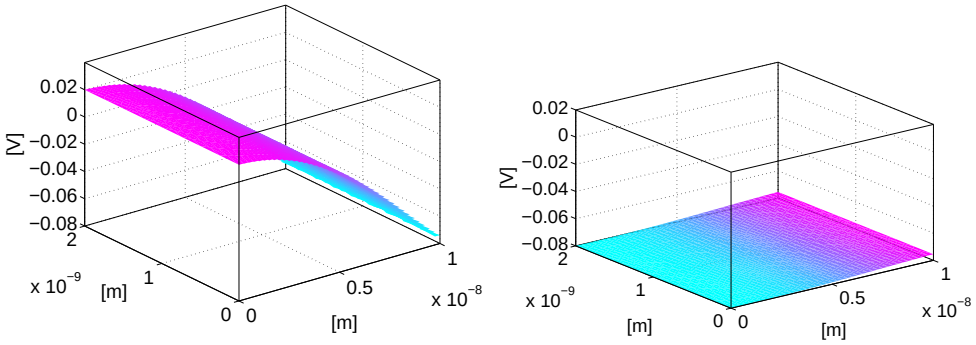

Figure 5: Electrochemical potential of a single K^+ channel.

5.2 I-V Characteristics with the PNP-ST Model

In this section, we perform a comparison between the full model and the sole PNP model on the same test case as in Sect. 5.1. In order to provide a quantitative estimate of the net contribution of the fluid-mechanical current to the total ionic flux density, we carry out two sets of numerical studies as a function of an external pressure drop $\Delta\,p_{4,2} = \overline{p}_4 - \overline{p}_2$, the varying parameter being the value of the ionic mobility μ. The main difficulty is the choice of proper pressure values on the external (Γ_2) and internal (Γ_4) sides of the channel. This is a nontrivial issue, because of the lack of precise specific data, except for those referring to osmotic pressure theory [14], which states that the pressure difference $\Delta p_{4,2}$ across the membrane is related to the difference between the chemical potentials of the electrolyte in the cytoplasm and in the cleft, and, as

consequence, of the corresponding ionic concentrations, according to the relation

$$\Delta p_{4,2} = q\, V_{th} \left([\mathrm{K}^+]_e - [\mathrm{K}^+]_i \right),$$

where $[\cdot]_e$ and $[\cdot]_i$ are the external and internal concentrations expressed in m^{-3} and $q = 1.602 \cdot 10^{-19}\, C$ is electron charge.

We start studying the I-V characteristics of the K^+ channel as a function of $\Delta p_{4,2}$ in the cases $\Delta p_{4,2} = 10\, bar$ (a) and $\Delta p_{4,2} = 50\, bar$ (b), with $\mu = 7.2 \cdot 10^{-8}\, m^2 V^{-1} s^{-1}$ as in Sect. 5.1, case (b) representing an extreme operating condition because typical values of $\Delta\, p_{4,2}$ are in the range $[1,\ 10]\, bar$. The results are illustrated in Fig. 6. In case (a), we notice that the computed

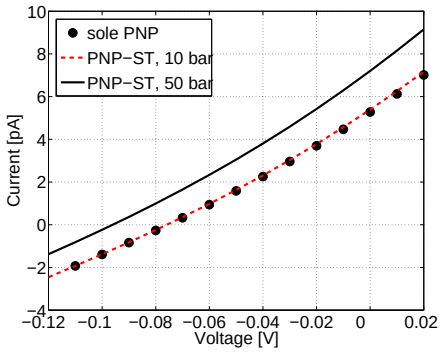

Figure 6: I-V curve as a function of pressure drop: $\Delta p_{4,2} = 10\, bar$ (dashed line), $\Delta p_{4,2} = 50\, bar$ (solid line). The black dots refer to the computation with the sole PNP model.

current (dashed line) is in excellent agreement with the analysis done using the sole PNP model (black dots). In case (b), the comparison between the PNP-ST model (solid line) with the sole PNP model (dashed line) demonstrates the importance of the Stokes fluid contribution to the ionic current flux.

Then, we study the I-V characteristics of the K^+ channel as a function of $\Delta p_{4,2}$ in the cases $\Delta p_{4,2} = 1\, bar$ (a), $\Delta p_{4,2} = 10\, bar$ (b) and $\Delta p_{4,2} = 50\, bar$ (c), with $\mu = 10^{-8}\, m^2 V^{-1} s^{-1}$. This modified value of the ionic mobility attempts to simulate:

1. an effective diffusion reduction due to the presence of narrowing regions (cf. Sect. 3.1 and Fig. 2);

2. the interionic interactions which have been neglected in Ref. [16].

The results are illustrated in Fig. 7. In case (a), we notice that the computed current (dotted

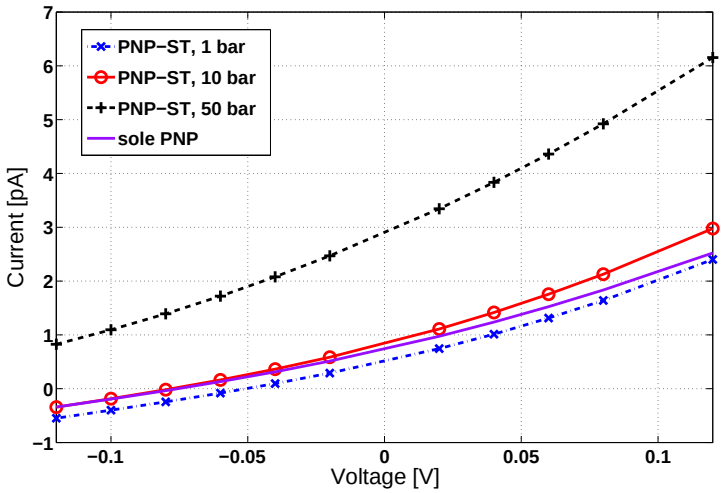

Figure 7: I-V curve as a function of pressure drop: $\Delta p_{4,2} = 1\,bar$ (asterisks), $\Delta p_{4,2} = 10\,bar$ (circles) and $\Delta p_{4,2} = 50\,bar$ (crosses). The solid line (without symbols) refers to the computation with the sole PNP model.

line) exhibits a significant deviation with respect to the computation with the sole PNP model (solid line, no symbols) for a negative value of the applied bias, whilst a similar behaviour can be noticed for the computed current in case (b) for a positive value of the applied bias (solid line, circles). These results demonstrate that the fluid forces significantly contribute to determine ionic transport in the channel and, as a consequence, to the total ionic current flux, for a wide range of admissible pressure drops. The fluid-mechanical contribution is furtherly enhanced in (the unrealistic) case (c), compared to the same simulation performed with the higher value of

the ionic mobility and reported in Fig. 6.

6 Conclusions and Future Perspectives

In this article, we have schematically illustrated a possible scenario for interdisciplinary description of complex systems in Human Sciences and Bio–Nanotechnologies.

The considered mathematical setting is based on a nonlinearly coupled system of partial differential equations, comprising a PNP model for the electro–chemical analysis, and a NS (ST) model for the fluid–mechanical part. Appropriate boundary and initial conditions have been supplied to the problem at hand, and suitable functional iteration techniques and computational finite element methodologies have been proposed to numerically solve the resulting equations. Models and algorithms have then been validated on the simulation of a realistic VOCs under several working conditions. The numerical results are:

1. in very good agreement with tabulated data and ranges predicted by theory and experimental measurements;

2. obtained with a dramatic reduction of computational time compared to the Molecular–Dynamics simulations of [8].

Forthcoming issues that we intend to investigate are:

- a more realistic description of the channel geometry, with possible full 3D computations. In particular, a more faithful definition of channel narrowing should automatically account for (effective) diffusion reduction, and, in turn, require the replacement of the ST model with the NS model;

- the inclusion of gating channel mechanisms, which should require including in the model

the elastic deformation of the membrane;

- the implementation of the reduced-order model proposed in [9], supplied with the quantitative evaluation of g_{ch} given by the present work, for the numerical simulation of the EOSFET device;

- the possibility of extending the use of the PNP-ST model to describe ionic flow in the electrolyte cleft;

- a mathematical analysis of the PNP/NS (ST) model (well-posedness, asymptotics and convergence of the functional iteration map and the related discretization schemes).

7 Acknowledgements

Bice Chini was supported by the Fondazione Cariplo Grant "New Targets For The Diagnosis and Prevention of Human Deseases: Genomics and Proteonics of GPCRs". Joseph W. Jerome was supported by ONR Subcontract LLCN00014-05-C-0241 (Advanced Tools for Computational Materials Engineering). Riccardo Sacco was supported by the M.U.R.S.T. Grant: Adattività Numerica e di Modello per Problemi alle Derivate Parziali (2005–2006).

References

[1] B. Alberts, A. Johnson, J. Lewis, M. Raff, K. Roberts, and P. Walter. *Molecular Biology of the Cell.* Garland Publishing, New York, 2002.

[2] V. Barcilon, D. Chen, R. Eisenberg, and J.W. Jerome. Qualitative properties of steady-state Poisson-Nernst-Planck systems: perturbation and simulation study. *SIAM J. Appl. Math.*, 57 (3):631–648, 1997.

[3] F. Brezzi, L.D. Marini, S. Micheletti, P. Pietra, R. Sacco, and S. Wang. Discretization of semiconductor device problem (i). In P.G. Ciarlet, W.H.A. Schilders, and E.J.W. ter Maten, editors, *Handbook of Numerical Analysis*, volume 13, pages 317–441. Elsevier North-Holland, Amsterdam, 2005.

[4] P. Causin and R. Sacco. A dual-mixed hybrid formulation for fluid mechanics problems: Mathematical analysis and application to semiconductor process technology. *Comput. Methods Appl. Mech. Engrg.*, 192:593–612, 2003.

[5] D.P. Chen, R.S. Eisenberg, J.W. Jerome, and C.-W. Shu. A hydrodynamic model of temperature change in open ionic channels. *Biophysics J.*, 69:2304–2322, 1995.

[6] B. Chini, J.W. Jerome, and R. Sacco. Multi-physics modeling and finite element approximation of charge flow in ionic channels. In L.J. Ernst, G.Q. Zhang, P. Rodgers, M. Meuwissen, S. Marco, and O. de Saint Leger, editors, *Proceedings of EUROSIME06 Conference, Como, Italy*, pages 153–160, Maastricht (The Netherlands), April 24 2006. IEEE Shaker Publishing.

[7] B. Cockburn, G. E. Karniadakis, and C.-W. Shu. The development of Discontinuous Galerkin methods. In B. Cockburn, G. E. Karniadakis, and C.-W. Shu, editors, *Lecture Notes in Computational Science and Engineering*, volume 11, pages 3–50. Springer, 2000.

[8] P.S. Crozier, D. Henderson, R.L. Rowley, and D.D. Busath. Model channel ion currents in Na–Cl-extended simple point charge water solution with applied–field molecular dynamics. *Biophysical J.*, 81:3077–3089, 2001.

[9] P. Fromherz. Neuroelectronics interfacing: Semiconductor chips with ion channels, cells and brain. In R. Weise, editor, *Nanoelectronics and Information Technology*, pages 781–

810. Wiley-VCH, Berlin, 2003.

[10] C. L. Gardner, W. Nonner, and R. S. Eisenberg. Electrodiffusion model simulation of ionic channels: 1d simulations. *Journal of Computational Electronics*, 3:25–31, 2004.

[11] B. Hille. *Ionic Channels of Excitable Membranes*, volume 17(1). Sinauer Associates, 1992.

[12] J.W. Jerome. *Analysis of Charge Transport.* Springer-Verlag, Berlin Heidelberg, 1996.

[13] G. Karniadakis, A. Beskok, and N. Aluru. *Microflows and Nanoflows. Fundamentals and Simulation*, volume 29 of *Interdisciplinary Applied Mathematics.* Springer–Verlag, New York, 2005.

[14] J. Keener and J. Sneyd. *Mathematical Physiology*, volume 8 of *Interdisciplinary Applied Mathematics.* Springer–Verlag, New York, 1998.

[15] C. Kittel. *Introduction to Solid State Physics.* Wiley, 1956.

[16] S. Koneshan, J.C. Rasaiah, R.M. Lynden-Bell, and S.H. Lee. Solvent structure, dynamics, and ion mobility in aqueous solutions at 25 C. *Journal of Physical Chemistry*, 102:4193–4204, 1998.

[17] L.D. Landau and E.M. Lifshitz. *Fluid Mechanics.* Butterworth–Heinemann, Oxford, 2000.

[18] P.A. Markowich. *The Stationary Semiconductor Device Equations.* Springer-Verlag, Wien-New York, 1986.

[19] S. Micheletti, R. Sacco, and F.Saleri. On some mixed finite element methods with numerical integration. *SIAM J. Sci. Comput.*, 23-1:245–270, 2001.

[20] E. Neher. Molecular biology meets microelectronics. *Nature Biotechnology*, 19:114, 2001.

[21] J.H. Park and J.W. Jerome. Qualitative properties of steady-state Poisson-Nernst-Planck systems: mathematical study. *SIAM J. Appl. Math.*, 57 (3):609–630, 1997.

[22] A. Quarteroni and A. Valli. *Numerical Approximation of Partial Differential Equations.* Springer-Verlag, New York, Berlin, 1994.

[23] A. Quarteroni and A. Valli. *Domain Decomposition Methods for Partial Differential Equations.* Oxford Science Publications, New York, 1999.

[24] I. Rubinstein. *Electro–Diffusion of Ions.* SIAM, Philadelphia, PA, 1990.

[25] B. Straub, E. Meyer, and P. Fromherz. Recombinant maxi-k channels on transistor, a prototype of iono-electronic interfacing. *Nature Biotechnology*, 19:121–124, 2001.